Relation Between Flow Enhancement Factor and Structure for Core-Softened Fluids Inside Nanotubes

José Rafael Bordin*

Programa de Pós-Graduação em Física, Instituto de Física, Universidade Federal do Rio Grande do Sul, Caixa Postal 15051, CEP 91501-970, Porto Alegre, RS, Brazil

Institut für Computerphysik, Universität Stuttgart, Almandring 3, 70569 Stuttgart, Germany

Alexandre Diehl[†]

Departamento de Física, Instituto de Física e Matemática, Universidade Federal de Pelotas, Caixa Postal 354, CEP 96010-900, Pelotas, RS, Brazil

Marcia C. Barbosa[†]

Instituto de Física, Universidade Federal do Rio Grande do Sul, Caixa Postal 15051, CEP 91501-970, Porto Alegre, RS, Brazil

ABSTRACT: The relationship between enhancement flow and structure of core-softened fluids confined inside nanotubes has been studied using nonequilibrium molecular dynamics simulation. The fluid was modeled with different types of attractive and purely repulsive two length scale potentials. Such potentials reproduce in bulk the anomalous behavior observed for liquid water. The dual control volume grand canonical molecular dynamics method was employed to create a pressure gradient between two reservoirs connected by a nanotube. We show how the nanotube radius affects the flow enhancement factor for each one of the interaction potentials. The connection between structural and dynamical properties of the confined fluid is discussed, and we show how attractive and purely repulsive fluids exhibit distinct behaviors. A continuum to subcontinuum flow transition was found for small nanotube radius. The behavior obtained for the core-softened fluids is similar to what was recently observed in all-atom molecular dynamics simulations for classical models of water and also in experimental studies. Our results are explained in the framework of the two length scale potentials.
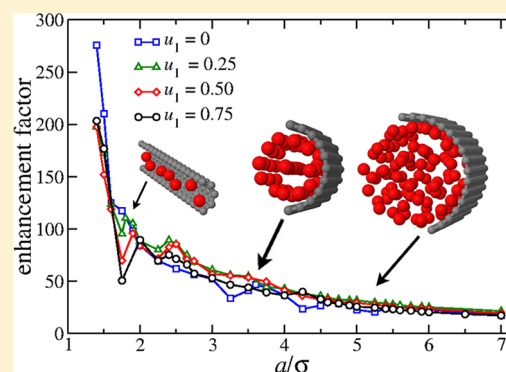
I. INTRODUCTION

Transport of fluids in the nanometer scale, particularly the flow of fluids through nanotubes (NTs), has received considerable attention over the past decade.[1] Nanotubes are nanostructures with a cylindrical shape, made of different materials and with extraordinary properties.[2] For instance, in diffusive processes, carbon and silicon-carbide nanotubes show a highly smooth potential energy landscapes that lead to a fast gas and liquid fluxes, higher than what was observed in other nanoporous materials.[3−9] This makes nanotubes a promising material for the production of nanoporous membranes with several technological applications, such as separation of fluid mixtures and water desalination, and with the capacity to mimic biological nanopores.[7,10−14]

The anomalous and fast flow in nanotubes and the possibility of achieving experimental regions, which in general are inaccessible in bulk experiments, make water one of the most studied confined liquids. For instance, experiments of confined water in nanotubes and nanopores are used to avoid the

spontaneous crystallization of water and to observe its hypothetical second critical point.[15−19] Despite these promising scientific applications, our main interests in this paper are the dynamical properties and their relation with the structure of the fluid inside the nanotube. In this case, one of the most interesting properties is the anomalous increase of the flow enhancement factor, defined as the ratio between the hydraulic conductivity, obtained from molecular simulations, and the hydraulic conductivity predicted by the classical continuum models, such as the Hagen−Poiseuille (HP) equation. Recent experiments[7,20,21] show that water has a flow enhancement factor several orders of magnitude higher than what is generally found from the classical flow theories. Also, they show a transition from continuum to subcontinuum flow.[21] Such behavior was observed not only for hydrophobic carbon

nanotubes, but also in hydrophilic alumina channels,[22] which seems that the flow enhancement is not an exclusive property of water. Ethanol, methane and decane flow also exhibit a huge enhancement in carbon nanotubes.[20,23]

Water, even in bulk, presents an anomalous behavior in many of its properties, such as density, diffusion, heat capacity, and others. Despite its molecular simplicity, the job to create a proper classical model for water is a huge task, mainly due to the temperature and pressure dependent hydrogen bonds, polarizability and the nonsymmetrical charge distribution. As a consequence, several classical models of water were already proposed for classical all-atom molecular dynamics (MD) simulations. There are more than 25 models of (bulk) water using empirical potentials, each one of then giving different values for the physical and chemical properties of water.[24] Nevertheless, these models were extensively applied to study the structural, dynamical and thermodynamic behavior of water in nanoconfinement.[25−38]

Different models of water can lead to significantly distinct results.[39] For structural properties, simulations of water inside (9,9) and (10,10) carbon nanotubes by Koles et al.[40] show an ordered water structure, while the simulations by Wang et al.[41] indicate a disordered structure. The behavior of the water self-diffusion D inside nanotubes is also still not clear. Some simulational studies indicate that D has a minimum value and an enhancement for small radius,[42−45] while other studies show a monotonically decreasing curve as we shrink the nanotube radius.[46−48]

Despite this, several simulational studies were performed to understand the flow enhancement factor of water in nanotubes. According to these simulations,[49−51] the flow has two distinct regimes: a continuum regime, described by the classical fluid dynamics, such as HP equation, and a subcontinuum regime, where the HP formulation fails because a discrete description of the system is necessary. Although Noy et al.[52] have suggested that this continuum to subcontinuum transition occurs when the fluid assumes a single file formation inside the nanotube, the explanation for this effect remains unclear.

One alternative to the classical models of water is the so-called two length scale potential fluids. Such water-like fluids are characterized by a simple potential model with two characteristic length scales and, despite the simplicity of the model, exhibits in bulk the thermodynamic, dynamic, and structural anomalies of water.[53−57] They also predict the existence of a second critical point hypothesized by Poole and collaborators for the ST2 water model.[58] This suggests that some of the unusual properties observed in water can be quite universal and possibly present in other systems.

These simple models offer some advantages when compared with all-atom models. For instance, using core-softened (CS) fluids modeled by two length scale potentials, it is possible to simulate large systems during long times at low computational costs. Therefore, it is possible to investigate a large region in the pressure versus temperature phase diagram. In addition, these effective potentials allow for studying universal properties that are not only present in water, but are also common to other systems, such as the thermodynamic anomalies also present in liquid metals, silica, silicon, graphite, Te, Ga, Bi, S, and BeF_2 and the diffusion anomaly also found in silica and silicon.

This is a indicative that some of the water properties attributed to its directionality can be found even in spherically symmetric systems. The drawback of the effective potentials is

that they lead to a qualitative comparison with experimental results, unlike all-atom models.

Recently these simple water-like models have been used to analyzed confined systems. Krott and Barbosa have shown that water-like anomalies remain present even when the fluid is confined between parallel plates.[59] Also, Bordin et al.[60] have performed equilibrium NpT MD simulations of CS fluids confined in nanotubes, showing that this fluid exhibits a minimum in the self-diffusion D, at a specific critical value for the nanotube radius, as we decrease the radius, an an anomalous increase for D below this critical value, when the fluid assumes a single file structure. This behavior is the same obtained in all-atom MD simulations of classical models of water.[42−45] Now it is our interest to verify whether these water-like fluids exhibit the continuum to subcontinuum flow transition observed for water in experiments and all-atom MD simulations.

In order to test this assumption, we have performed nonequilibrium MD simulations to study the enhancement factor of CS fluids. We modeled two kinds of water-like fluids: one purely repulsive[56,57] and another attractive, with three different depths for the attractive well.[61] First, we verify whether these fluid models are capable of capturing the continuum to subcontinuum transition observed for water, as well as the flow enhancement factor. Next, we analyze how the layering and structuring of the fluid inside the nanotube affect the flow. Also, the distinct flow and structural behavior due to the existence of the attractive tail in the potential are discussed.

The paper is organized as follow. The water-like fluid, nanotube model and the details of the simulational methods used in our calculations are presented in section II. Next, we discuss our results in section III, and the conclusions are summarized in section IV.

II. THE MODEL AND THE SIMULATION DETAILS

A. The Model. Four different potentials for the water-like fluid were used in our simulations: one purely repulsive, and three with an attractive well. In all cases, the fluid was modeled as a collection of spherical particles with diameter σ and mass m, interacting through the interaction potential described by the equation bellow:[61]

$$\frac{U(r_{ij})}{\varepsilon} = 4\left[\left(\frac{\sigma}{r_{ij}}\right)^{12} - \left(\frac{\sigma}{r_{ij}}\right)^6\right] + u_0 \exp\left[-\frac{1}{c_0^2}\left(\frac{r_{ij}-r_0}{\sigma}\right)^2\right]$$
$$- u_1 \exp\left[-\frac{1}{c_1^2}\left(\frac{r_{ij}-r_1}{\sigma}\right)^2\right] \tag{1}$$

where $r_{ij} = |\vec{r}_i - \vec{r}_j|$ is the distance between two fluid particles i and j. This equation has three terms: the first one is the standard 12−6 Lennard-Jones (LJ) potential,[62] the second one is a Gaussian centered at r_0/σ, with depth $u_0\varepsilon$ and width $c_0\sigma$, and the last term is also a Gaussian, but centered at r_1/σ, with depth $u_1\varepsilon$ and width $c_1\sigma$, responsible for the attractive tail of the potential. Using only the first Gaussian with $u_0 = 5.0$, $c_0 = 1.0$, and $r_0 = 0.7$, eq 1 represents a purely repulsive two length scale potential, as indicated in Figure 1 by the solid line for $u_1 = 0$. Adding the second Gaussian with different values for u_1 the potential shows an attractive well, which changes the pressure phase diagram for this fluid.[56,57,61] Also, it is known from previous works that these CS fluids exhibit thermodynamic, dynamic, and structural anomalies similar to the anomalies
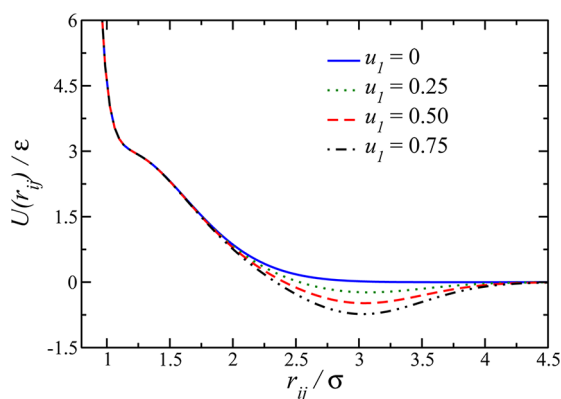
Figure 1. Interaction potential between two fluid particles as a function of their separation for several values of attractive depth u_1.

present in water[63,64] and an anomalous increase in diffusion when confined in a nanotube.[60] In our simulations we have used the parameters $u_0 = 5.0$, $c_0 = 1.0$, $r_0 = 0.7$, $c_1 = 0.5$, $r_1 = 3.0$ and $u_1 = 0$, 0.25, 0.5, and 0.75. The resulting shape for the interaction potential is shown in Figure 1.

We investigate the dynamical behavior of this fluid flowing from one reservoir, named control volume 1 (CV_1) on the left, to another reservoir, the control volume 2 (CV_2) on the right, through a nanotube. The simulation box, a parallelepiped with dimensions $L_x \times L \times L$ in the x, y, and z directions, respectively, containing the reservoirs-nanotube setup, is illustrated in Figure 2. The box size in the x-direction was fixed in $L_x = 50\sigma$, while L
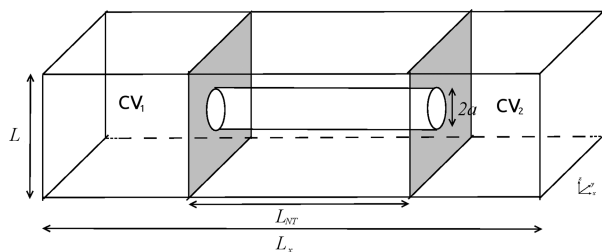
Figure 2. Schematic depiction of the simulation cell with the nanotube and reservoirs. The cylindrical nanotube in the center has radius a and length L_{NT}.

$= 10\sigma$ for the y and z directions for nanotubes with radius $a < 4\sigma$ and $L = 2a+2\sigma$, otherwise. The tube structure was constructed as a wrapped sheet of LJ particles with diameter $\sigma_{NT} = \sigma$. Nanotube atoms and water-like particles interact through a purely repulsive Weeks−Chandler−Andersen (WCA) potential[62]

$$U^{WCA}(r_{ij}) = \begin{cases} U_{LJ}(r_{ij}) - U_{LJ}(r_c), & r_{ij} \leq r_c \\ 0, & r_{ij} > r \end{cases} \quad (2)$$

Here, U_{LJ} is the standard 12−6 LJ potential, included in the first term of eq 1, and $r_c = 2^{1/6}\sigma$ is the usual cutoff for the WCA potential. Also, the term r_{ij} measures the distance between a fluid particle i and a fixed nanotube atom j. Surrounding the nanotube entrances, two repulsive walls are placed, as shown by the two gray planes in Figure 2. In order to represent the interaction between a fluid particle and these flat repulsive walls, we can use the same WCA eq 2. To this end, we have to consider r_{ij} in that equation as the distance between the wall

position and the x-coordinate of the fluid particle. In this case, the cutoff r_c assumes the same value as before.

B. The Simulation Details. We employ the dual control volume grand canonical molecular dynamics (DCV-GCMD) method[14,65,66] to generate a steady state flow of particles from the CV_1, with higher fluid density, to the CV_2, with a lower density. The DCV-GCMD technique allows us to fix the density inside the control volumes using a hybrid MD and grand canonical Monte Carlo (GCMC) method. The initial density in both two control volumes are fixed at the desired value using the GCMC simulation, and then evolved in time using standard NVT MD simulations. To restore the densities in both reservoirs to their initial values, we alternate the MD steps with GCMC steps, realized only inside the two control volumes shown in Figure 2. In our simulations we performed 150 GCMC steps at each 500 MD steps. This ratio between MD and GCMC steps ensures that the densities inside the control volumes fluctuate less than 1% before being restored by GCMC.

The system temperature was fixed at $k_B T/\varepsilon = 1.0$, using a Nose−Hoover heat-bath with a coupling parameter $Q = 2$. At this temperature the bulk system is far away from the anomaly region for all fluids we are simulating. Periodic boundary conditions were applied in all directions. For simplicity, we assume that the nanotube atoms are fixed (i.e., not time integrated) during the simulation. A time step of $\delta t = 0.005$, in LJ time units,[62] was used.

The fluid−fluid interaction, eq 1, has a cutoff radius $r_{cut}/\sigma = 4.5$ for all cases. The nanotube radius was varied from $a/\sigma = 1.4$ to $a/\sigma = 7.0$, and in all simulations the tube length was fixed in $L_{NT}/\sigma = 15$. The initial densities in the left and rigth reservoirs were fixed at $\rho_1\sigma^3 = 0.1$ and $\rho_2\sigma^3 = 0.01$, respectively, using a standard GCMC simulation in each reservoir, during 5×10^5 steps, with the initial velocity for each particle obtained from a Maxwell−Boltzmann distribution at the desired temperature. After that, we performed 5×10^5 DCV-GCMD steps in order to obtain a steady state flux of particles between the two reservoirs. This steady state is the initial time for the production of our results, during 5×10^7 DCV-GCMD steps, where 10 independent runs were averaged to evaluate the properties of the fluid inside the nanotube at the same initial conditions.

Recent computational[9,50,51] and experimental[21] studies suggest that if the flow enhancement factor does not have a monotonic behavior as we vary the nanotube radius, and if there is a discontinuous region, the system exhibits a transition from continuum to subcontinuum transport. Also, this information allows us to say when the flow of this CS fluid is described by the HP equation, and when the flow is enhanced. According to the HP equation, the flow rate of a Newtonian fluid inside a cylinder of radius a is given by

$$v_x = 2\langle v_x \rangle \left[1 - \left(\frac{r_\rho}{a} \right)^2 \right] \quad (3)$$

where $r_\rho = (y^2 + z^2)^{1/2}$ is the Euclidian distance from the x-axis in cylindrical coordinates, and $\langle v_x \rangle$ is the average velocity, described by

$$\langle v_x \rangle = \gamma_{HP} \frac{\Delta p}{L_{NT}} \quad (4)$$

where Δp is the pressure gradient and γ_{HP} is the hydraulic conductivity,[9] defined by

$$\gamma_{HP} = \frac{a^2}{8\eta} \tag{5}$$

for a given viscosity η. We can express the results from the DCV-GCMD simulations in a similar form of eq 5 using

$$\langle v_x \rangle = \gamma_{MD} \frac{\Delta p}{L_{NT}} \tag{6}$$

where γ_{MD} is the hydraulic conductivity obtained from the MD results. The flow enhancement factor is then defined as

$$\varepsilon = \frac{\gamma_{MD}}{\gamma_{HP}} \tag{7}$$

To evaluate γ_{HP}, we have performed NpT simulations defined in our previous work,[60] and obtained the diffusion coefficient D_x from the Green–Kubo relation,

$$D_x = \frac{1}{N} \sum_{i=1}^{N} \int_0^\infty \langle v_{x,i}(t) \cdot v_{x,i}(0) \rangle \, dt \tag{8}$$

where N is the total number of particles and $v_{x,i}(t)$ is the axial velocity of particle i at time t. The bracketed quantity represents the autocorrelation function. The viscosity was then estimated using the Einstein equation,

$$\eta = \frac{k_B T}{3\pi\sigma D_x} \tag{9}$$

where k_B is the Boltzmann constant.

III. RESULTS AND DISCUSSION

A. Case A: CS Fluid with Attractive Tail. In Figure 3 we illustrate the flow enhancement factor as a function of the
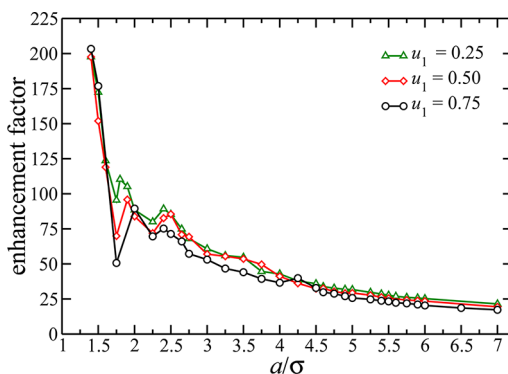
Figure 3. The flow enhancement factor as function of the nanotube radius, for CS fluids with an attractive tail depth u_1.

nanotube radius for $u_1 = 0.25$, 0.5, and 0.75. For a nanotube radius larger than $a/\sigma = 4.5$, the flow enhancement factor increases monotonically when the radius is decreased, for all attractive well depths shown in Figure 3. This indicates that in this region, a continuum description of the system is still valid.[51] At the limit of very large radius, the enhancement factor saturates (not shown in Figure 3). For a nanotube with a radius in the region $2.5 \leq a/\sigma \leq 4.0$, the curves feature small oscillations, specially when $u_1 = 0.25$ and $u_1 = 0.5$. This behavior is not observed for the standard 12−6 LJ fluids. For a nanotube with a radius smaller than $a/\sigma = 2.5$, the curves show large oscillations, followed by a sharp increase. Such fluctuations are related to the structural changes of the fluid,

from a disordered bulk-like to an ordered solid-like structure and then to a single file, as we will show hereafter.

Our results show oscillations similar to the oscillations observed for the TIP5P model of water confined in carbon nanotubes,[51] SPC/E water confined in silicon-carbide nanotubes,[9] and experiments.[21] However, while for these simulations and experiments only one minimum at small radius was observed, for our water-like model we found two well-defined minima, at $a/\sigma = 1.75$ and $a/\sigma = 2.25$. Also, the values of the enhancement factor ε for our CS model are smaller than the obtained for water inside carbon and silicon-carbide nanotubes.[9,21,50,51]

In order to identify what in our potential can be modified to achieve a larger enhancement factor, we analyze the attractive well depth u_1. As we can see in Figure 3, as the depth of the attractive well is decreased, the enhancement factor is increased. It is easier for the particles to jump from one length scale to another one when u_1 is not too deep, leading to an enhancement of the flow for small radius. As we will show in section IIIB, in the limit of $u_1 = 0$, these oscillations will vanish. For the larger depth, $u_1 = 0.75$, although no oscillations were found in region $2.5 \leq a/\sigma \leq 4.0$, as illustrated in Figure 3, the fluctuations in region $1.75 \leq a/\sigma \leq 2.25$ are much stronger than the other values of u_1.

In order to understand the origin of the oscillations observed in the enhancement flow as illustrated in Figure 3, the structure of particles inside the nanotube was analyzed. In bulk solution this CS fluid exhibits a high ordering, with a huge impact on the dynamical properties,[61] while for LJ fluids this layering is not observed. Under strong confinement, like inside nanotubes, this ordering and consequential changes in the structure of the fluid, induced by the interaction with the nanotube walls, leads to fluctuations in the flow. To understand the relation between the structure and the flow in our confined water-like fluid, we analyze in Figure 4 the different structures formed for several values of radius, and in Figure 5 the radial fluid density distribution for the respective values of a/σ. For wide radius, $a/\sigma = 7.0$, the fluid exhibits a shell of particles around the nanotube walls, and at the nanotube center it behaves has a disordered bulk-like fluid, as shown in Figures 4A and 5A. Hence, we have two regimes: one structured and well-defined near the walls, and another diffuse in the nanotube center. When we shrink the nanotube, the walls compress the fluid, and, as a result, it becomes more structured. When the radius is decreased to $a/\sigma = 4.5$ the fluid presents a well-defined structure, with two concentric cylindrical layers: one near the wall, and another around the x-axis, as shown in Figures 4B and 5B. This layering leads to small oscillations in the flow enhancement factor curve, which become stronger as we decrease the value of u_1. Also, when this layering occurs continuum theories fail to describe properly the system, since the properties of the nanotube walls and the structure of the fluid play a major role.

As we continue to decrease the radius, new structures are formed. For $a/\sigma = 3.5$, as shown in Figures 4C and 5C, the cylindrical central layer becomes a line, while for $a/\sigma = 2.5$ the central layer vanishes, and only one layer is observed, as shown in Figures 4D and 5D. When we decrease the radius even more, there is no space for the particles to stand at an energetically favorable distance. In other words, they cannot stay near at one of the characteristic length scale of our potential. Hence, the well structured layer becomes a disordered layer when $a/\sigma = 2.25$, as shown in Figures 4E and 5E, which leads the flow
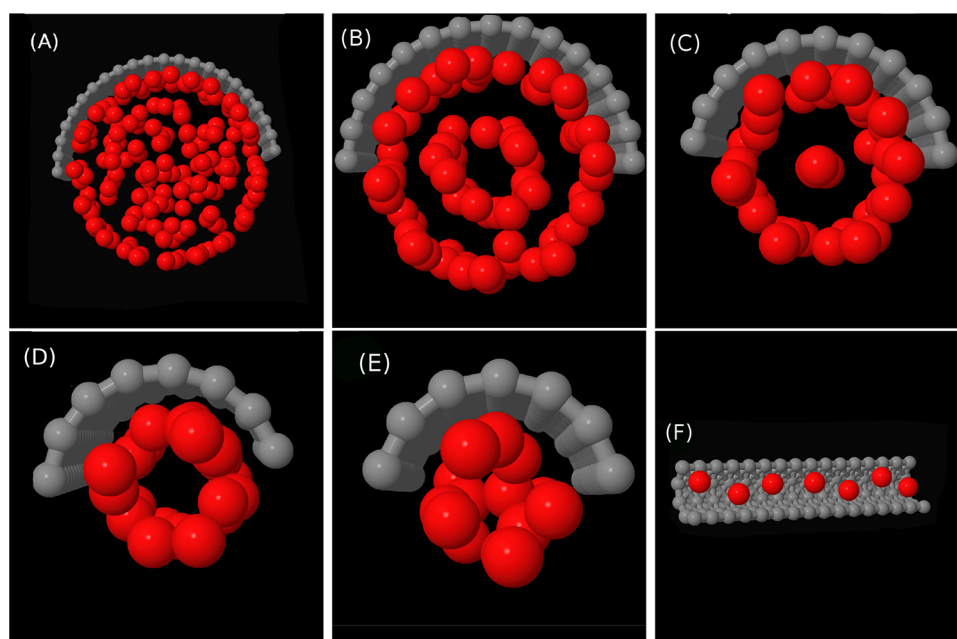
Figure 4. Snapshots of the system show the change of the fluid structure as we decrease the nanotube radius: $a/\sigma = 7.0$ (A), 4.5 (B), 3.5 (C), 2.5 (D), 2.25 (E) and 1.5 (F). For better visualization, only fluid particles (red) inside the nanotube and half of the nanotube (gray) are shown. Only the results for the $u_1 = 0.5$ are shown, since the behavior for the other attractive cases is similar. The snapshots were taken with the Jmol package.[67]
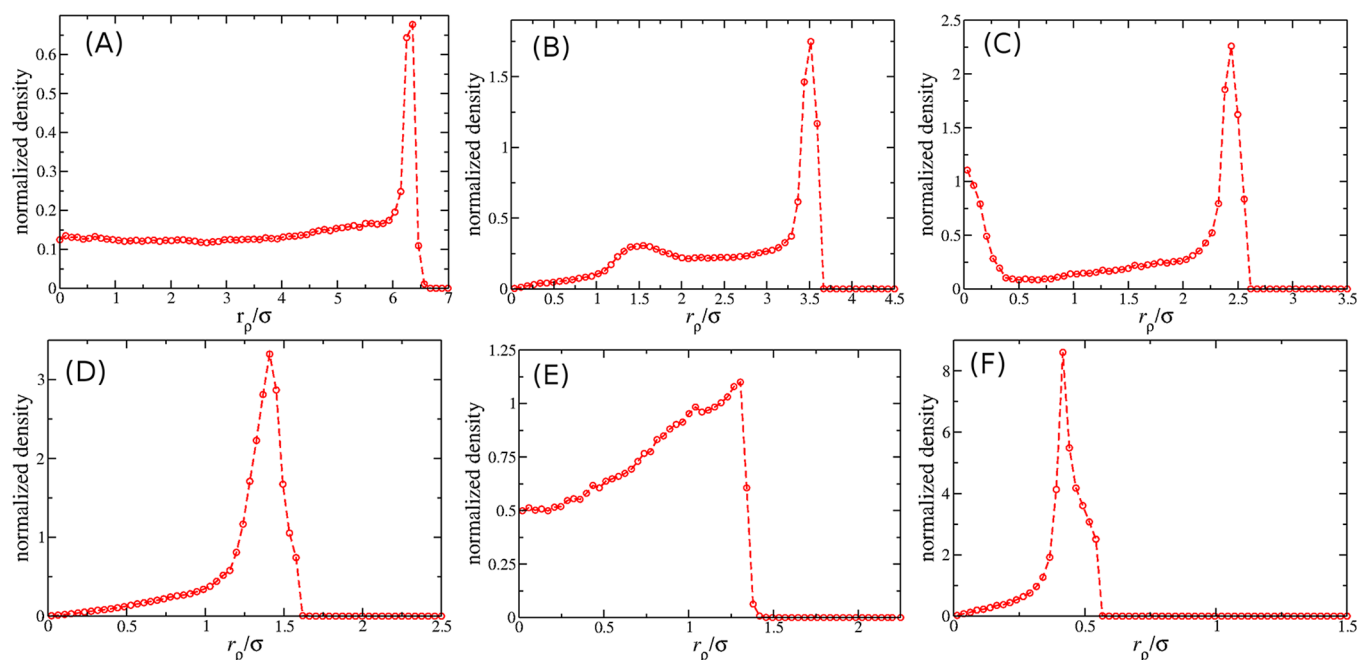

Figure 5. Normalized density of fluid particles inside the nanotube for several values of nanotube radius: $a/\sigma = 7.0$ (A), 4.5 (B), 3.5 (C), 2.5 (D), 2.25 (E), and 1.5 (F). Only the results for the $u_1 = 0.5$ are shown, since the behavior for the other attractive cases is similar.

enhancement factor to the first minimal value. Reducing the nanotube radius to smaller values makes the fluid modify its structure to a single file, as shown in Figures 4F and 5F. This transition leads to a new minimal value and then to an increase in ε for small radius.

The layering formation is a result of the competition between the fluid–fluid interaction, eq 1, and the fluid–nanotube interaction, eq 2. For radius $a/\sigma > 2.25$, the system minimizes the energy forming layers. Also, for large radius, the entropic contribution for the free energy is dominated by enthalpic effects.[60] For $a/\sigma < 1.75$, there is only one layer of particles,

and, due to the repulsive fluid-wall interaction, the particles can move faster and "free" in the flow direction. This raises the entropy, which becomes dominant. The attractive interaction between the fluid particles leads to a region where the competition between enthalpy and entropy is stronger, $1.75 \leq a/\sigma \leq 2.25$. This becomes clear if we consider that in this region the effective available diameter for the fluid, $d_{eff} = 2a - \sigma_{NT}$, is $2.5 \leq d_{eff}/\sigma \leq 3.5$. Therefore, the fluctuations occur in a region where the repulsive walls obligate the fluid to stay in a distance where the attractive well is deeper, and we have a competition for the particles whether to stay ordered, with a
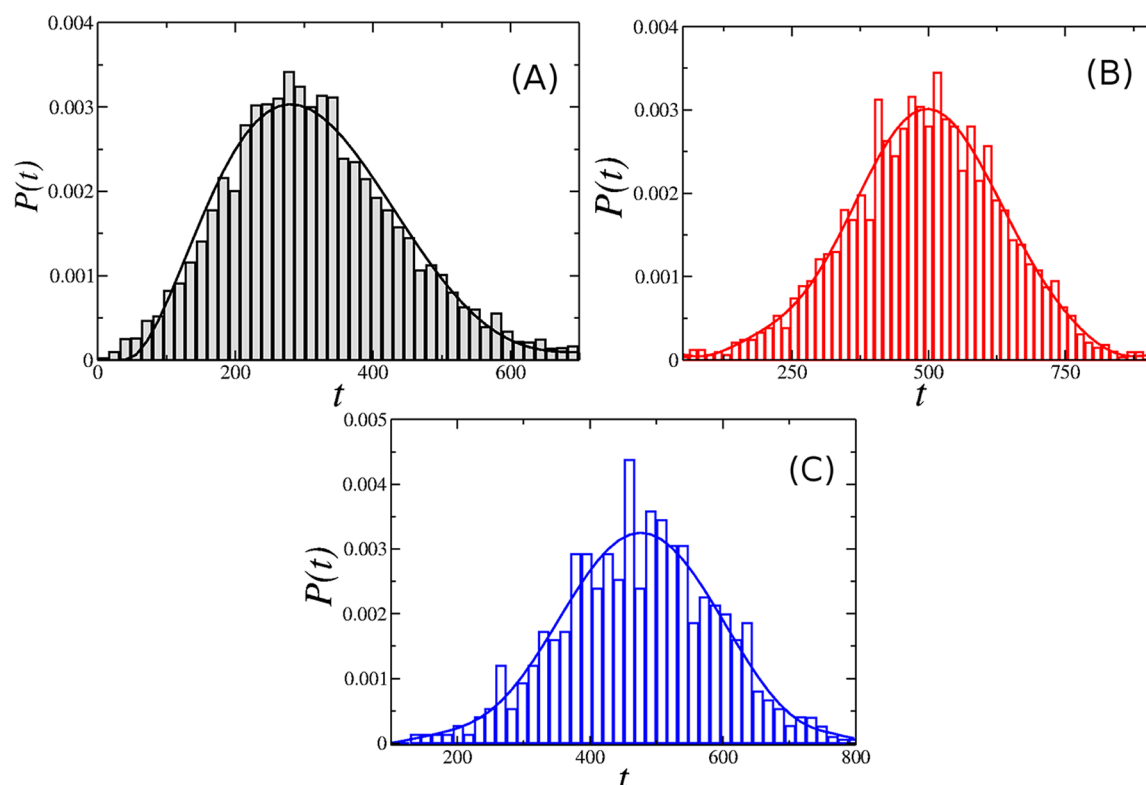
Figure 6. Mean first passage time $P(t)$ distribution for attractive CS fluid as function of the nanotube radius: $a/\sigma = 7.0$ (A), $a/\sigma = 4.5$ (B) and $a/\sigma = 2.5$ (C). A Gaussian-like distribution was observed in all three cases. Only the results for the $u_1 = 0.5$ are shown, since the behavior for the other attractive cases is similar.

lower mobility in an energetically favorable distance, or to stay in an energetically unfavorable distance, but with a higher mobility. These results indicate a transition from continuum to subcontinuum transport for attractive CS particles inside nanotubes. In order to understand the collective movement of the fluid particles, we evaluate the distribution $P(t)$ of the mean first passage time (MFPT) of particles through the nanotube. The MFPT distribution $P(t)$ measures the probability that a fluid particle crosses the nanotube in a time t. Analysis of the MFPT distribution $P(t)$ shows that all layers move at the same velocity. In Figure 6 we can see that the $P(t)$ distribution has a Gaussian-like shape, indicating that even when the system exhibits two layers, both move at the same mean velocity. This collective motion occurs due to the attractive tail of the potential, as we will show in the next section.

B. Case B: Purely Repulsive CS Fluid. Now we address the question of what is the effect of the presence of an attractive term in the fluid potential on the flow enhancement factor. Let us first analyze the flow enhancement factor, shown in Figure 7, for the purely repulsive potential case, $u_1 = 0$ in eq 1. Unlike the previous case, we do not observe minimum values in the enhancement factor for nanotubes with small radius, $a/\sigma < 2.25$, only oscillations in region $3.0 \leq a/\sigma \leq 4.5$ that are larger than the fluctuations present for the attractive potentials. This indicates that this fluid also exhibits a transition from continuum to subcontinuum transport. Therefore, these fluctuations and changes in the shape of the enhancement factor curve are also connected to the structural properties of the confined fluid.

Analyzing the different fluid structures inside the nanotube shown in Figures 8 and 9, we can see that this system exhibits a
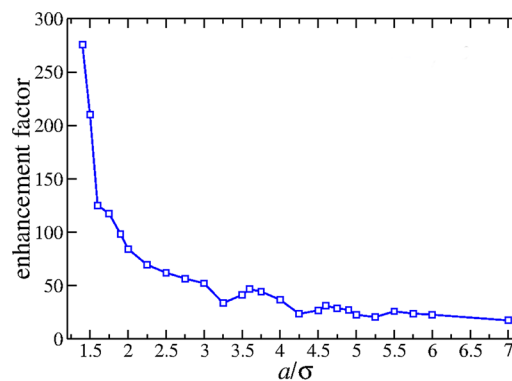

Figure 7. The flow enhancement factor as a function of the nanotube radius, for a purely repulsive CS fluid, $u_1 = 0$.

well-defined layering even for a wide radius. While in the attractive case the fluid inside the nanotube with $a/\sigma = 7.0$ shows a disordered bulk-like structure, the same kind of behavior for nonattractive fluids was observed only for larger values of radius, $a/\sigma = 10.0$, as the snapshot of Figure 8A and the density profile of Figure 9A show. For $a/\sigma = 7.0$, the snapshot and density distribution analysis (Figures 8B and 9B), indicate the existence of three concentric layers. The main reason for this is the absence of an attractive well in the potential model. Now, the fluid assumes a layered structure at a well-defined distance even for spacious channels. When $a/\sigma = 7.0$, the distance between the layers is approximately 2σ, which is one of the characteristic lengths of our potential. Since there is no attractive part, the particles will remain in the layers to stay in the minimum of energy. In other words, the attractive tail increases the entropy for nanotubes with wide radius,
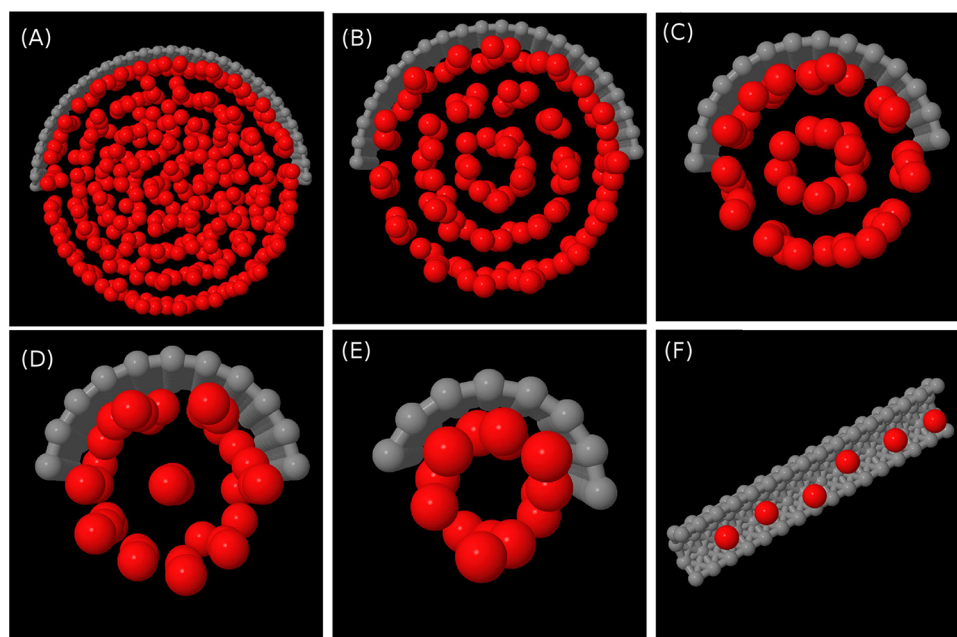
Figure 8. Snapshots of the system composed by a purely repulsive CS fluid shows the variation of the structure as we shrink the nanotube radius: a/σ = 10 (A), 7 (B), 4.5 (C), 3.5 (D), 2.25 (E), and 1.75 (F). For better visualization, only the fluid particles (red) inside the nanotube and half of the nanotube (gray) are shown. Snapshots taken with the package Jmol.[67].
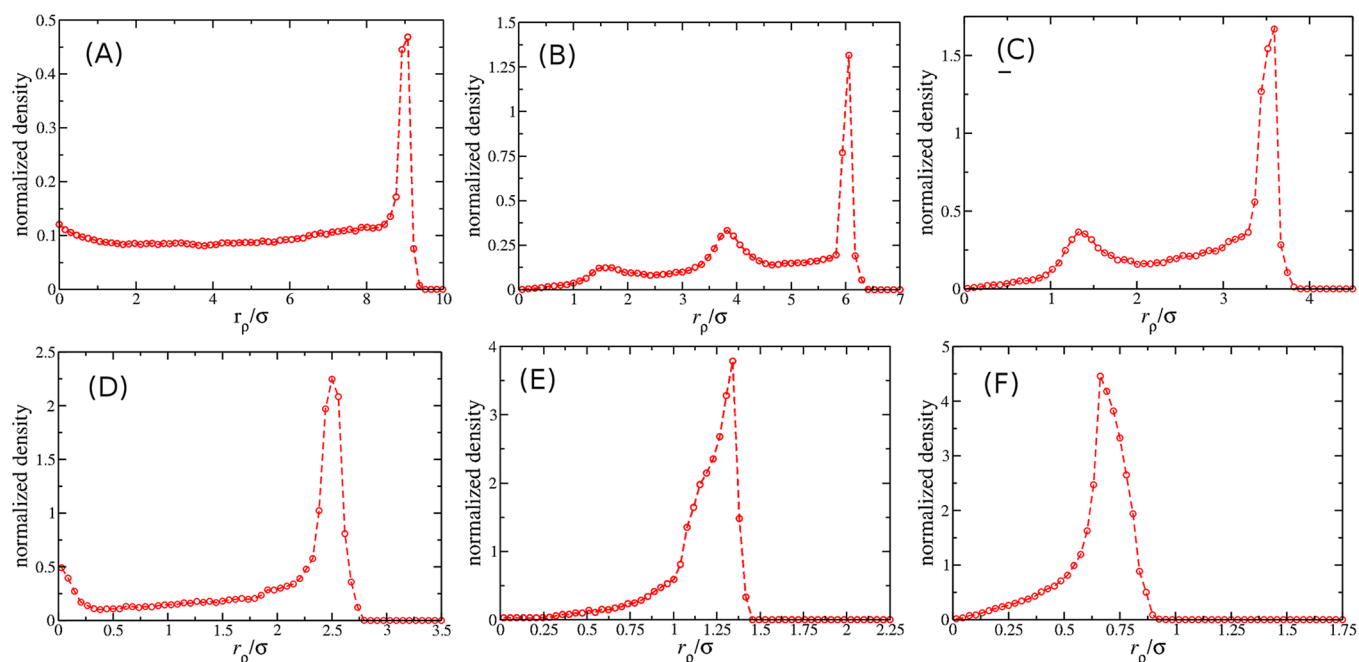
Figure 9. Normalized density fluid particles inside the nanotube for several values of nanotube radii: a/σ = 10.0 (A), 7.0 (B), 4.5 (C), 3.5 (D), 2.25 (E), and 1.75 (F).

leading the fluid to assume a bulk-like structure in the center. Meanwhile, when the attractive tail is not present, the fluid assumes a solid-like ordering. For smaller radius, the structure inside the nanotube changes from a triple to a double cylindrical layer, according to Figures 8C and 9C, then a central line of particles surrounded by a cylindrical layer (Figures 8D and 9D, and finally one single cylindrical layer, as shown in Figures 8E and 9E. This is the same structural behavior observed in the attractive case, and all changes in the fluid conformation occur when the flow enhancement factor exhibits a fluctuation. When $a/\sigma < 2.0$, a single file of particles is

observed, as shown in Figures 8F and 9F. Unlike the previous case, the purely repulsive water-like fluid does not have a disordered structure in region $1.75 \leq a/\sigma \leq 2.25$, as shown in Figures 8E and 9E, and, consequentially, the flow enhancement factor curve does not exhibits any discontinuity in this region. Once the system is purely repulsive, the particles change their distances from one characteristic length to another more easily, leading to a smoother curve. This confirms our assumption for the attractive case, namely, the fluctuations for small radius are due to the attractive tail in the potential and will be stronger for deeper attractive wells.
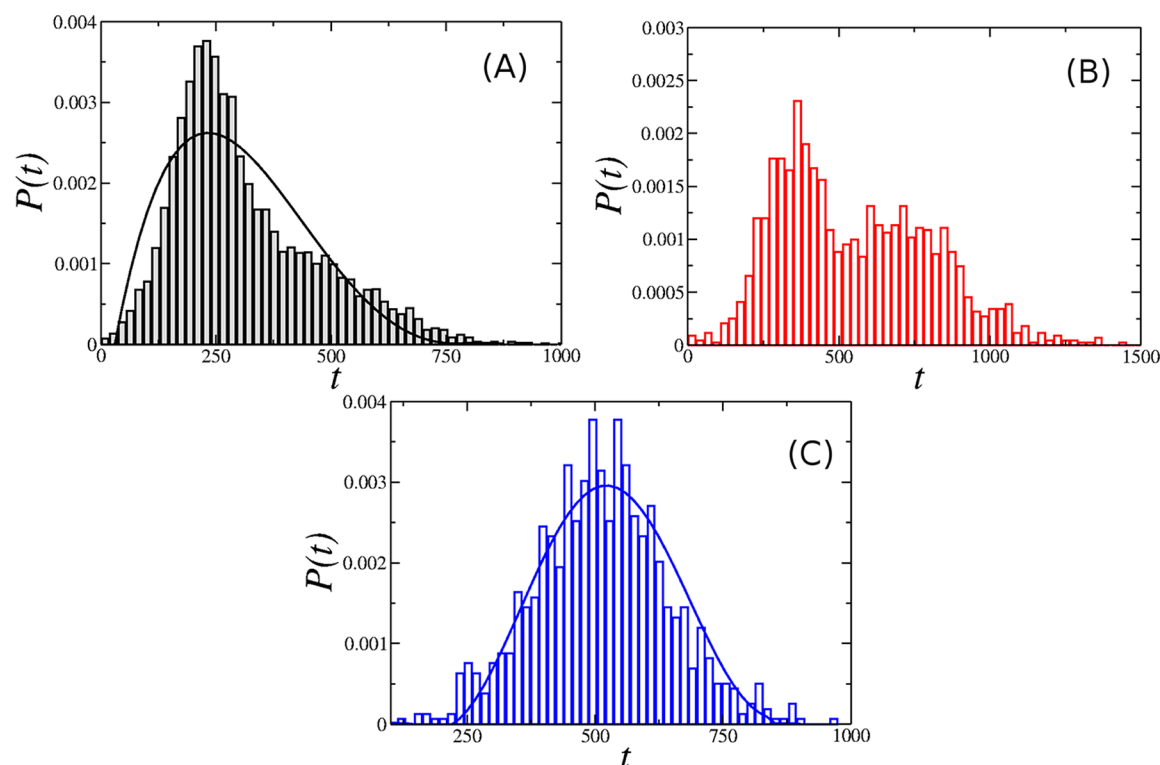
Figure 10. Mean first passage time distribution $P(t)$ for purely repulsive fluid as we decrease the nanotube radius: from a Poisson-like shape in $a/\sigma = 7.0$ (A), to a distribution with two distinct peaks in $a/\sigma = 4.5$ (B) and a Gaussian-like distribution in $a/\sigma = 2.5$ (C).

Finally, the investigation of the MFPT $P(t)$ distribution for the nonattractive system indicates that the fluid layers move at different velocities. As we show in Figure 10A for $a/\sigma = 7.0$, or three layers inside the nanotube in Figure 8B, the distribution has a Poisson-like shape. This is a consequence of the friction between the external layer and the nanotube walls, which leads the particles of this layer to move slower than the particles in the central layer. For the double layer case, the difference between the velocity of the central and the external layer is even clearer. In Figure 10B we show the case $a/\sigma = 4.5$, with two distinct peaks, one due to the faster inner layer and another due to the slower external layer. For smaller radius, when the system has only one layer, the distribution assumes a Gaussian-like shape, as shown in Figure 10C.

IV. CONCLUSION

The connection between flow enhancement, structure, and potential model for CS fluids confined inside nanotubes was studied in this paper. We have performed DCV-GCMD simulations of a water-like fluid flowing through a nanotube. The fluid was modeled using four kinds of spherically symmetric two length potential, and the nanotube was modeled as fixed hard spheres. Our systems exhibit a transition from continuum to subcontinuum flow, featured by fluctuations and a large growth in the enhancement factor curve for small nanotube radius, similar to the enhancement observed for water. This effect arises from changes in the structural properties of the fluid, produced by the competition between the fluid-nanotube interaction and the fluid–fluid interaction. This competition generates correlated layers, and different structures were observed. For wide nanotubes we observe a bulk-like structure for attractive potentials and a solid-like structure with three layers for the purely repulsive case. For

narrow channels, other structures were observed: double cylindrical layers, a central line surrounded by a cylindrical layer, one single cylindrical layer and, for narrow channels, a single file. The transition from single cylindrical layer to a single file depends on the shape of the potential. For the potential with an attractive tail, the system exhibits a disordered structure between these ordered structures. On the other hand, for the purely repulsive case, this transition is from a cylindrical layer to a single file.

In addition, we have found that the layers move all together for attractive systems, while for repulsive fluids the layers exhibit different flow velocities. Our results indicate that the presence of a transition from continuum to subcontinuum transport, strongly connected to the structural properties of the fluid when confined, is also a property of spherically symmetric systems. For these systems we do not expect any directionality. Therefore, our results indicate that this is not only a property of directional systems, like water.

■ AUTHOR INFORMATION

Corresponding Author
*E-mail: bordin@if.ufrgs.br.

Notes
The authors declare no competing financial interest.
†E-mail: diehl@ufpel.edu.br (A.D.); marcia.barbosa@ufrgs.br (M.C.B.).

■ REFERENCES

(1) Karniadakis, G. E.; Beskok, A.; Aluru, N. R. *Microflows and Nanoflows - Fundamentals and Simulation*; Springer Science+Business Media, Inc.: New York, 2005.

(2) Valentin, N. P. Carbon nanotubes: Properties and application. *Mater. Sci. Eng. R.* **2004**, *43*, 61−102.

(3) Papadopoulos, K. Influence of orientational ordering transition on diffusion of carbon dioxide in carbon nanopores. *J. Chem. Phys.* **2001**, *114*, 8139−8145.

(4) Mao, Z.; Sinnot, S. B. Predictions of a Spiral Diffusion Path for Nonspherical Organic Molecules in Carbon Nanotubes. *Phys. Rev. Lett.* **2002**, *89*, 278301.

(5) Ackerman, D. M.; Skoulidas, A. I.; Sholl, D. S.; Johnson, J. K. Diffusivities of Ar and Ne in Carbon Nanotubes. *Mol. Simul.* **2003**, *29*, 677−684.

(6) Skoulidas, I.; Sholl, D. S.; Johnson, J. K. Adsorption and diffusion of carbon dioxide and nitrogen through single-walled carbon nanotube membranes. *J. Chem. Phys.* **2006**, *124*, 054708.

(7) Holt, J. K.; Park, H. G.; Wang, Y. M.; Stadermann, M.; Artyukhin, A. B.; Grigoropulos, C. P.; Noy, A.; Bakajin, O. Fast mass transport through sub-2-nanometer carbon nanotubes. *Science* **2006**, *312*, 1034−1035.

(8) Striolo, A. The mechanism of water diffusion in narrow carbon nanotubes. *Nano Lett.* **2006**, *6*, 633−639.

(9) Khademi, M.; Sahimi, M. Molecular dynamics simulation of pressure-driven water flow in silicon-carbide nanotubes. *J. Chem. Phys.* **2011**, *135*, 204509.

(10) Shen, H. MD simulations on the melting and compression of C, SiC and Si nanotubes. *J. Mater. Sci.* **2007**, *42*, 6382−6387.

(11) Zhang, Y.; Huang, H. Stability of single-wall silicon carbide nanotubes - Molecular dynamics simulations. *Comput. Mater. Sci.* **2008**, *43*, 664−669.

(12) Elimelech, M.; Philip, W. A. The future of seawater desalination: Energy, technology, and the environment. *Science* **2011**, *333*, 712−717.

(13) Hilder, T. A.; Gordon, D.; Chung, S. H. Computational modeling of transport in synthetic nanotubes. *Nanomedicine* **2011**, *7*, 702−709.

(14) Bordin, J. R.; Diehl, A.; Barbosa, M. C.; Levin, Y. Ion fluxes through nanopores and transmembrane channels. *Phys. Rev. E* **2012**, *85*, 031914.

(15) Liu, L.; Chen, S. H.; Faraone, A.; Yen, C. W; Mou, C. Y. Pressure dependence of fragile-to-strong transition and a possible second critical point in supercooled confined water. *Phys. Rev. Lett.* **2005**, *95*, 117802.

(16) Mallamace, F.; Branca, C.; Corsaro, C.; Leone, N.; Spooren, J.; Stanley, H. E.; Chen, S. H. Dynamical crossover and breakdown of the Stokes−Einstein relation in confined water and in methanol-diluted bulk water. *J. Phys. Chem. B* **2010**, *114*, 1870−1878.

(17) Chen, S. H.; Mallamace, F.; Mou, C. Y.; Broccio, M.; Corsaro, C.; Faraone, A.; Liu, L. The violation of the Stokes−Einstein relation in supercooled water. *Proc. Natl. Acad. Sci. U.S.A.* **2006**, *103*, 12974−12978.

(18) Lombardo, T. G.; Giovambattista, N.; Debenedetti, P. G. Structural and mechanical properties of glassy water in nanoscale confinement. *Faraday Discuss.* **2008**, *141*, 359−376.

(19) Stanley, H. E.; Buldyrev, S. V.; Kumar, P.; Mallamace, F.; Mazza, M. G.; Stokely, K.; Xu, L.; Franzese, G. Water in nanoconfined and biological environments: (Plenary Talk, Ngai-Ruocco 2009 IDMRCS Conf.). *J. Non-Cryst. Solids* **2011**, *357*, 629−640.

(20) Majumder, M.; Chopra, N.; Andrews, R.; Hinds, B. J. Nanoscale hydrodynamics: Enhanced flow in carbon nanotubes. *Nature* **2005**, *438*, 44−45.

(21) Qin, X.; Yuan, Q.; Zhao, Y.; Xie, S.; Liu, Z. Measurement of the rate of water translocation through carbon nanotubes. *Nano Lett.* **2011**, *11*, 2173−2177.

(22) Lee, K. P.; Leese, H.; Mattia, D. Water flow enhancement in hydrophilic nanochannels. *Nanoscale* **2012**, *4*, 2621−2627.

(23) Whitby, M.; Thanou, M.; Cagnonand, L.; Quirke, N. Enhanced fluid flow through nanoscale carbon pipes. *Nano Lett.* **2008**, *8*, 2632−2637.

(24) Chaplin, M. Water models. http://www.lsbu.ac.uk/water/models.html (accessed Feb 20, 2013).

(25) Rovere, M.; Gallo, P. Effects of confinement on static and dynamical properties of water. *Eur. Phys. J. E* **2003**, *12*, 77−81.

(26) Brovchenko, I.; Geiger, A.; Oleinikova, A.; Paschek, D. Phase coexistence and dynamic properties of water in nanopores. *Eur. Phys. J. E* **2003**, *12*, 69−76.

(27) Giovambattista, N.; Rossky, P. J.; Debenedetti, P. G. Phase transitions induced by nanoconfinement in liquid water. *Phys. Rev. Lett.* **2009**, *102*, 050603.

(28) Han, S.; Choi, M. Y.; Kumar, P.; Stanley, H. E. Phase transitions in confined water nanofilms. *Nat. Phys.* **2010**, *6*, 685−689.

(29) de los Santos, F.; Franzese, G. Understanding diffusion and density anomaly in a coarse-grained model for water confined between hydrophobic walls. *J. Phys. Chem. B* **2011**, *115*, 14311−14320.

(30) Gallo, P.; Rovere, M.; Chen, S.-H. Water confined in MCM-41: A mode coupling theory analysis. *J. Phys.: Condens. Matter* **2012**, *24*, 064109.

(31) Strekalova, E. G.; Mazza, M. G.; Stanley, H. E.; Franzese, G. Hydrophobic nanoconfinement suppresses fluctuations in supercooled water. *J. Phys.: Condens. Matter* **2012**, *24*, 064111.

(32) Melillo, M.; Zhu, F.; Snyder, M. A.; Mittal, J. Water transport through nanotubes with varying interaction strength between tube wall and water. *J. Phys. Chem. Lett.* **2011**, *2*, 2978−2983.

(33) de la Llave, E.; Molinero, V.; Scherlis, D. A. Water filling of hydrophilic nanopores. *J. Chem. Phys.* **2010**, *133*, 034513.

(34) de la Llave, E.; Molinero, V.; Scherlis, D. A. Role of confinement and surface affinity on filling mechanisms and sorption hysteresis of water in nanopores. *J. Phys. Chem. C* **2012**, *116*, 1833−1840.

(35) Zangi, R.; Mark, A. E. Monolayer Ice. *Phys. Rev. Lett.* **2003**, *91*, 025502.

(36) Zangi, R.; Mark, A. E. Bilayer ice and alternate liquid phases of confined water. *J. Chem. Phys.* **2003**, *119*, 1694−1700.

(37) Koga, K.; Gao, G. T.; Tanaka, H.; Zeng, X. C. Formation of ordered ice nanotubes inside carbon nanotubes. *Nature* **2001**, *412*, 802−805.

(38) Koga, K.; Gao, G. T.; Tanaka, H.; Zeng, X. C. How does water freeze inside carbon nanotubes? *Physica A* **2002**, *314*, 462−469.

(39) Alexiadis, A.; Kassinos, S. Influence of Water Model and Nanotube Rigidity on the Density of Water in Carbon Nanotubes. *Chem. Eng. Sci.* **2008**, *63*, 2093−2097.

(40) Kolesnikov, A. I.; Long, C. K.; de Souza, N. R.; Burnham, C. J.; Moravsky, A. P. Anomalously soft dynamics of water in carbon nanotubes. *Physica B: Condens. Matter* **2006**, *385*, 272−274.

(41) Wang, J.; Zhu, Y.; Zhou, J.; Lu, X. H. Diameter and helicity effects on static properties of water molecules confined in carbon nanotubes. *Phys. Chem. Chem. Phys.* **2004**, *6*, 829−835.

(42) Mash, R. J.; Joseph, S.; Aluru, N. R. Anomalously immobilized water: A new water phase induced by confinement in nanotubes. *Nano Lett.* **2003**, *3*, 589−582.

(43) Zhang, H.; Ye, H.; Zheng, Y.; Zhang, Z. Prediction of the viscosity of water confined in carbon nanotubes. *Microfluid. Nanofluid.* **2010**, *10*, 403−414.

(44) Farimani, A. B.; Aluru, N. R. Spatial diffusion of water in carbon nanotubes: From fickian to ballistic motion. *J. Phys. Chem. B* **2011**, *115*, 12145−12149.

(45) Zheng, Y.; Ye, H.; Zhang, Z.; Zhang, H. Water diffusion inside carbon nanotubes: mutual effects of surface and confinement. *Phys. Chem. Chem. Phys.* **2012**, *14*, 964−971.

(46) Liu, Y. C.; Shen, J. W.; Gubbins, K. E.; Moore, J. D.; Wu, T.; Wang, Q. Diffusion dynamics of water controlled by topology of potential energy surface inside carbon nanotubes. *Phys. Rev. B* **2008**, *77*, 125438.

(47) Nanok, T.; Artrith, N.; Pantu, P.; Bopp, P. A.; Limtrakul, J. Structure and dynamics of water confined in single-wall nanotubes. *J. Phys. Chem. A* **2009**, *113*, 2103−2108.

(48) Liu, Y.; Wang, Q.; Zhang, L. Fluid structure and transport properties of water inside carbon nanotubes. *J. Chem. Phys.* **2005**, *123*, 234701.

(49) Hummer, G.; Rasaiah, J. C.; Noworytra, J. P. Water conduction through the hydrophobic channel of a carbon nanotube. *Nature (London)* **2001**, *414*, 188−190.

(50) Thomas, J. A.; Macgaughey, A. J. H. Reassessing fast water transport through carbon nanotubes. *Nano Lett.* **2008**, *8*, 2788−2793.

(51) Thomas, J. A.; Macgaughey, A. J. H. Water flow in carbon nanotubes: Transition to subcontinuum transport. *Phys. Rev. Lett.* **2009**, *102*, 184502.

(52) Noy, A.; Park, H. G.; Fornasiero, F.; Holt, J. K.; Grigoropoulos, C. P; Bakajin, O. Nanofluidics in carbon nanotubes. *Nano Today* **2001**, *2*, 22−29.

(53) Jagla, E. A. Phase behavior of a system of particles with core collapse. *Phys. Rev. E* **1998**, *58*, 1478−1486.

(54) Yan, Z.; Buldyrev, S. V.; Giovambattista, N.; Stanley, H. E. Structural order for one-scale and two-scale potentials. *Phys. Rev. Lett.* **2005**, *95*, 130604.

(55) Xu, L.; Kumar, P.; Buldyrev, S. V.; Chen, S.-H.; Poole, P.; Sciortino, F.; Stanley, H. E. Relation between the Widom line and the dynamic crossover in systems with a liquid−liquid phase transition. *Proc. Natl. Acad. Sci. U.S.A.* **2005**, *102*, 16558−16562.

(56) de Oliveira, A. B.; Netz, P. A.; Colla, T.; Barbosa, M. C. Thermodynamic and dynamic anomalies for a three-dimensional isotropic core-softened potential. *J. Chem. Phys.* **2006**, *124*, 084505.

(57) de Oliveira, A. B.; Netz, P. A.; Colla, T.; Barbosa, M. C. Structural anomalies for a three dimensional isotropic core-softened potential. *J. Chem. Phys.* **2006**, *125*, 124503.

(58) Poole, P. H.; Sciortino, F.; Essmann, U.; Stanley, H. E. Phase behaviour of metastable water. *Nature (London)* **1992**, *360*, 324−328.

(59) Krott, L.; Barbosa, M. C. Anomalies in a waterlike model confined between plates. *J. Chem. Phys.* **2013**, *139*, 084505.

(60) Bordin, J. R.; de Oliveira, A. B.; Diehl, A.; Barbosa, M. C. Diffusion enhancement in core-softened fluid confined in nanotubes. *J. Chem. Phys.* **2012**, *137*, 084504.

(61) da Silva, J. N.; Salcedo, E.; de Oliveira, A. B.; Barbosa., M. C. Effects of the attractive interactions in the thermodynamic, dynamic and structural anomalies of a two length scale potential. *J. Chem. Phys.* **2010**, *133*, 244506.

(62) Allen, P.; Tildesley, D. J. *Computer Simulation of Liquids*; Oxford University Press: Oxford, U.K., 1987.

(63) Kell, G. S. Precise representation of volume properties of water at one atmosphere. *J. Chem. Eng. Data* **1967**, *12*, 66−69.

(64) Angell, C. A.; Finch, E. D.; Bach, P. Spin−echo diffusion coefficients of water to 2380 bar and 20 °C. *J. Chem. Phys.* **1976**, *65*, 3063−3066.

(65) Heffelfinger, G. S.; Van Smol, F. Diffusion in Lennard-Jones fluids using dual control volume grand canonical molecular dynamics simulation (DCV-GCMD). *J. Chem. Phys.* **1994**, *100*, 7548−7552.

(66) Thompson, A. P.; Ford, D. M.; Heffelfinger, G. S. Direct molecular simulation of gradient-driven diffusion. *J. Chem. Phys.* **1998**, *109*, 6406−6114.

(67) Milischuk, A. A.; Ladanyi, B. M. *Jmol: An open-source java viewer for chemical structures in 3D*. 2011. Available online at jmol.org.